



MODIFICATION OF THE BAND GAP OF NANO TITANIUM DIOXIDE, ITS APPLICATION AND EFFECTIVENESS ON PHOTO DEGRADATION OF ORGANIC POLLUTANTS

Seenaa Wdaah Al Salih¹, Moatasem Al Salih^{2*} and Syakirah Samsudin³

¹The General Directorate of Education, Dhi Qar Governorate, Iraq.

^{3,2*}Biology department, Faculty of Science and Mathematics, University Pendidikan Sultan Idris (UPSI), Tanjung Malim Perak, Malaysia.

Abstract

This study aimed to modify the TiO₂ (anatase) band gap by doping with the platinum element using a sol-gel manner. Adaptation will diminish the gap separating energy altitudes between conduction band CB and valance band VB hence facilitating the transfer of excited electrons from VB to CB. Absorption of the energy from incident photons having the same or larger than the energy of the bandgap will promote the formation of the couple (electron-hole). The resulting (e⁻/h⁺) couple will act to produce (OH) radicals. OH radicals has a powerful capacity to destroy organic pollutants that a doped on the surface of the photocatalytic TiO₂. The arrangement of prepared TiO₂ powders was dulcified using XRD, The particle size and their distribution were characterized using Atomic Force Microscopy (AFM). The photocatalytic reaction was followed out using ATR-FTIR, UV-Vis spectrophotometry. The effect of the weight of the photocatalytic catalyst (TiO₂) from (0.10 – 0.83 g.L⁻¹) was studied to monitor its effect on the rate of decomposition of Phenanthrene on pre-determined aqueous solution of the compound. The most effective weight was found to equal (0.43 g.L⁻¹). The activities of TiO₂ (anatase) and doped TiO₂ with platinum were studied under the influence of source of UV light and direct sunlight under the same conditions. The results revealed that the reaction obeys first-order kinetics having a rate constant of 4.69×10⁻⁶ min⁻¹ for TiO₂ and 9.44×10⁻⁶ min⁻¹ for doped TiO₂.

Key words: Pt-doped-TiO₂, sol-gel method, photo degradation, photo catalysis, AFM, XRD.

Introduction

Titanium dioxide (TiO₂) defined as semi-conductor photo cataleptics chememulti properties for wide range applications include medical, Agricultural physiotherapist, industrial¹, sensors e.g. perform to be the utmost attracting funds for environmental disinfection. The main down side of TiO₂ semiconductor is that it retains a little segment of the sun-powered range in the UV vision (band gap energy of anatase TiO₂ is 3.20eV, 384nm and 3.02 eV, 411nm, for rutile TiO₂). Henceforward, to harvest so as to gather greatest sun powered vitality, it is basic to move the absorbing limit towards noticeable district (Gaya& Abdullah, 2008; Chen, & Mao, 2007; Chatterjee, & Dasgupta, 2005). Along these lines, the adjustment of TiO₂ to deliver its affectability to obvious light got one of the most significant objectives to expand the utility of TiO₂. Various techniques have been proposed to achieve

this explanation. Earlier assessments investigated the doping of progress metals of Ag, Zn and Cr into TiO₂, which can build the assimilation of obvious light, yet these doped materials experience the ill effects of warm precariousness and an expanded number of transporter recombination cores (Klosek, & Raftery 2001). In recent times, the doping of experimental atoms particles such as N (Asahi, R.*et al.*, 2001; Bozza, *et al.*, 2008), S (Umebayashi, *et al.*, 2003) and C (Khan., Al-Shahry, & Ingler, 2002), add to TiO₂. There are three altered main estimations concerning modify- faction applications of TiO₂ doped by Pt (Comini *et al.*, 2000; Mohapatra, Misra, Mahajan & Raja, 2007; Guayaquil-Sosa *et al.*, 2017).

1. Band gap reduction establish Pt. 2p state hybrids with O 2p states in anatase TiO₂ doped with platinum because their energies are very adjacent and consequently the band gap of TiO₂-pt. is contracted which

***Author for correspondence** : E-mail : moatasemalsalih@gmail.com, p20161001028@siswa.upsi.edu.my

make particles able to absorb energy visible light (Li, *et al.*, 2008; Sakai, *et al.*, 2008).

2. Earned Impurities energy scale quantified that TiO₂ oxygen atom positions substituted by platinum atom form remote impurity energy scales above the valence band. Exposure the sample by UV vision stimulates electrons in both the VB and the impurity imperativeness vitality of energy levels, but illumination with obvious light only excites electrons in the impurity energy stage (Hashimoto, Irie & Fujishima, A. 2005).

3. Oxygen vacancies concluded that oxygen-deficient sites formed in the grain boundaries are important to emerge via-activity and platinum doped in part of oxygen-deficient sites are important as a blocker for reoxidation (Gust, Momoda, Evans, & Mecartney, 2001).

Pollutants likes PAHs were shaped from the unfinished pyrolysis and combustion of organic compounds for example apply oil, petroleum gas, coal and wood which are usually recycled in energy producing (Joner, Leyval & Colpaert, 2006; Vela *et al.*, 2012) Which have a strong tendency to be adsorbed on the solid particles, particularly on the organic elements of the soil, the reason that's of their hydrophobic environmental processing (Bispo, Jourdain & Jauzein, 1999).

Furthermore, it's with high capacity to resistance persistently in the environmental factor due to their as influence to biological degradation. Consequently, numerous scholars have generously compensated regard for the experimental what in transit on which to take out PAHs and decrease their poisonousness (Godoi *et al.*, 2004; Wan *et al.*, 2006).

First of all, focusing on phenanthrene, it is a PAH composed of three fused benzene rings table 1. It is found in cigarette smoke and is a known irritant, photosensitizing skin to light. Phenanthrene appears as a white powder and insoluble in water but soluble in most organic solvents. Second, regarding benz [a] anthracene, it is one of the PAHs, consisting of a consecutive four-member ring structure as shown in table 2. It is natural products produced by the incomplete combustion of the organic material. The toxic effects of benz [a] anthracene and similar PAHs are primarily directed toward tissues that contain proliferating cells (Nisbet & Lagoy, 1992; Yan, *et al.*, 2004; Incardona *et al.*, 2006). (Endnotes)

Thus, current research aims to study how to dispose this toxic compound widespread in nature and agricultural soils and increased soil fertility by effectiveness on photo degradation Nano Titanium Dioxide doped with Platinum.

Photo catalysts, Pt-doped TiO₂, were prepared by

the sol-gel method. Initially, 5.00 ml of 35% ammonia solution as a platinum source was continually added into 10.00 ml titanium (IV) tetraisopropoxide as a titania precursor under the constantly stirring rate (400 rpm) at 303 K. In the first ten minutes of the addition, the rapid hydrolysis and condensation reactions caused more condensed solution, like colloids (Xie, *et al.*, 2017). This system was held for an hour at 303 K. Subsequently, yellow gel powder was obtained and then dried at 393 K in the oven for an hour to evaporate the remaining ammonia solution and some organic by-products generating from the hydrolysis reaction (Lam, Sin & Mohamed, 2008). Finally, as-prepared Pt-doped TiO₂ was calcined in the muffle furnace at various temperatures (573 K – 1173 K) for an hour to bring about a thermal decomposition, phase transition and removal of a volatile fraction. The color of Pt-doped TiO₂ much more varied depending upon the calcination temperature (Kryukova *et al.*, 2007; Patil *et al.*, 2019).

The decreasing concentration of phenanthrene was followed by measuring the absorption on a Perkin Elmer Lambda 35 spectrophotometer operated from 500 nm to 200 nm with slit width 2 nm. Distilled water was considered as a blank setup (Kumaravel *et al.*, 2019).

Use The sol-gel technique in modification the band gap semi-conductors such as TiO₂. General framework

Table 1: Constructions and principle characterized of phenanthrene and benz''a'' anthracene.

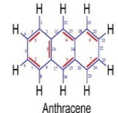
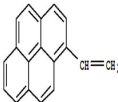
Structure	Molecular Formula	Molecular weight (g/mol)	Melting point (K)	Boiling point (K)
	C14H10	178.23	372.2	613
	C18H12	228.29	158	438

Table 2: optimized band gap energy (E_g).

Category of catalyst	λ (nm)	E _g (Joules) x10-19	E _g (eV)
TiO ₂ (anatase)	385	5.3	3.2
Pt-doped TiO ₂	483	4.2	2.4

Table 3: The initial rate of phenanthrene photo degradation at various TiO₂ loading.

Total (g.L ⁻¹)	0.10	0.25	0.35	0.43	0.51
%P.D.E	75	83	86	95	94
Amount (g.L ⁻¹)	0.59	0.68	0.76		0.82
%P.D.E	91	93	94		92

for usage sol- gel patterns is to “dissolve” the composites in an aquatic media in reformation in solid status in a stranded modus again. sol-gel method adaptable lets the fabrication of mighty oxide composites, also some non-oxides and hybrid organic-inorganic materials. appear in the mixture at the molecular with pure purity, melting temperature point wasn't unnecessary, establish a dense network of various compounds may be accomplished at normal temperatures. meager or thin films were coated, monoliths, composites, porous layers, powders and filaments. no requirement for exceptional or costly gear (Yin *et al.*, 2008).

The initial step of photo catalysis is the adsorption of photons by a molecule to produce highly reactive electronically excited states. The photon needs to have energy of ($h\nu$) equal to or more than the band gap energy of the semiconductor. The energy absorbed will cause an electron to be excited from the valence band to the conduction band, leaving a positive hole in the valence band. This movement of electrons forms (e^-/h^+) or negatively charged electron/positively charged hole pairs. The positively charged holes in valence band are powerful oxidants, whereas the negatively charged electrons in conduction band are good reductants (Li *et al.*, 2012). The free electrons and holes transform the surrounding oxygen or water molecules into $\cdot\text{OH}$ free radicals with super strong oxidization. It can oxygenolyse various kinds of organic compounds and some parts of minerals. It may also deoxidize harmful substances like benzene, formaldehyde and ammonia into CO_2 and water free of poison, harm and odor (Souza & Alves, (2020). Fig. 1.

Materials and Methods

Photo catalysts, Pt-doped TiO_2 , were prepared by the sol-gel method. Initially, 5.00 ml of with a purity of 99%. Hexachloroplatinic (IV) acid ($\text{H}_2\text{PtCl}_6\text{H}_2\text{O}$, Pt P 37.0%) was used as Pt precursor and supplied by Sinoparm Chemical Rengent Co., Ltd. Ethanol (99.7%) and nitric acid (65–68%) solution as a platinum⁽¹⁵⁾ source

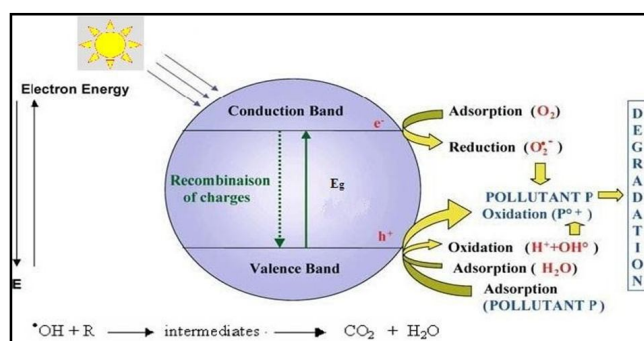


Fig. 1: The principle of TiO_2 photocatalysis. (Souza, & Alves, 2020).

was continually added into 10.00 ml titanium (IV) tetraisopropoxide as a titania precursor under the constantly stirring rate (400 rpm) at 303 K. In the first ten minutes of the addition, the rapid hydrolysis and condensation reactions caused more condensed solution, like colloids. This system was held for an hour at 303 K. Subsequently, yellow gel powder was obtained and then dried at 393 K in the oven for an hour to evaporate the remaining platinum solution and some organic by-products generating from the hydrolysis reaction (Brack, Dann, & Wijayantha, 2015; Zhu 2016) Finally, as-prepared Pt-doped TiO_2 was calcined in the muffle furnace at various temperatures (573 K – 1173 K) for an hour to bring about a thermal decomposition, phase transition and removal of a volatile fraction. The color of Pt-doped TiO_2 much more varied depending upon the calcination temperature (Xie *et al.*, 2017).

XRD

Regardless of whether you are working with thin tape, slender films, Nano-materials, powders or fluids, the Smart Lab will give good outcome the usefulness to make the estimations need to make when need to make them and proven in nanoparticles framework a Holland Philips X pert X-ray powder diffraction (XRD) diffracted meter using monochromatic high-intensity Cu K, radiation ($\lambda = 0.154056 \text{ nm}$), at a scanning speed of $2^\circ/\text{min}$ from 10° to 60° (2θ).

AFM

AFM for the fastest pathway to inventive study, produces Park NX10 information which can be proven, recreate and distribute at the most elevated nano targets. From test setting to full sweep imaging, estimation and investigation, Park NX10 spares you time at all times. It is an apparatus to determine diameters for residues, molecules and particles, aimed to determination the particles size in three dimension x, y and z, beside distribution of this atoms. Angstrom A advanced Inc. USA . Model scanning probe microscope a.a.3000A.

ATR-FTIR, UV-V

Attenuated total reflection (ATR) is an inspecting strategy utilized related to infrared spectroscopy which empowers tests to be analyzed straightforwardly in the strong or fluid state without further planning, ATR-FTIR Bruker Model Tensor 27, UV- Visible Spectrophotometer, PG instrument Ltd, double+90Plus.

Results and Discussion

Evaluation Characterization of synthesizing nanocomposite to distinguish the synthesized nano- TiO_2 (anatase) and nano- Pt doped TiO_2 residues or particles,

XRD and AFM were verified were considered by a Philips Xpert X-ray powder diffraction (XRD) diffractometer. as demonstration in Fig. (2-a, b) by associating with the typical outcome, the x-ray diffraction indicated. Fig. 2-a X-ray diffraction for TiO_2 (anatase) from the layout the main peak noticed at $2\theta = 25.3543$ the intensity is 100% and peaks at $2\theta = 38.7298, 47.0871, 53.9206, 55.1004$. Fig. 2-b epitomize a XRD for Pt. -doped TiO_2 , the top peak noticed at ($2\theta = 25.7175$) with intensity 100 % other peaks at $2\theta = 38.15221, 47.4960, 54.2079, 55.3687$.

TiO_2 AFM spectra specified to the dimension distribution of particles in sites between (60- 135nm), for TiO_2 (anatase form), the size distribution of particles sites, located between (50- 150nm), for Pt doping TiO_2 of prepared at 873k. which is the outcomes demonstrated that Pt- doped TiO_2 has the largest surface area, followed TiO_2 (anatase) has the lowest surface region contrasted and diminishing molecule sizethat illustrate in following

figures:

Atr-Ftir Spectrum

The outcome demonstrated in Fig. 5 shows that Low-frequency bands located in 500cm^{-1} go to the vibration of the Ti–O– Ti bond for induction TiO_2 (anatase) as in Fig 5.

Also, the results are shown In Fig. 6. of catalyst Pt doped with TiO_2 and heat at $120\text{C}\text{\ae}\%$ temperature for remove H_2O residues and dried the powder so that appear the main peaks around 3243 to 1633 cm^{-1} that can be hypothecated to the water and hydroxyl groups, The peak at 1438cm^{-1} could be altered to the platinum atoms substitute into TiO_2 network, This peak belong the Pt-H bending (Reszczynska *et al.*, 2012).

UV-Vis absorptionspectra

UV-visible spectra indicated wavelength eventuate the absorption of the induced by Pt doped with TiO_2 which represents marker the boundary of the alignment in the

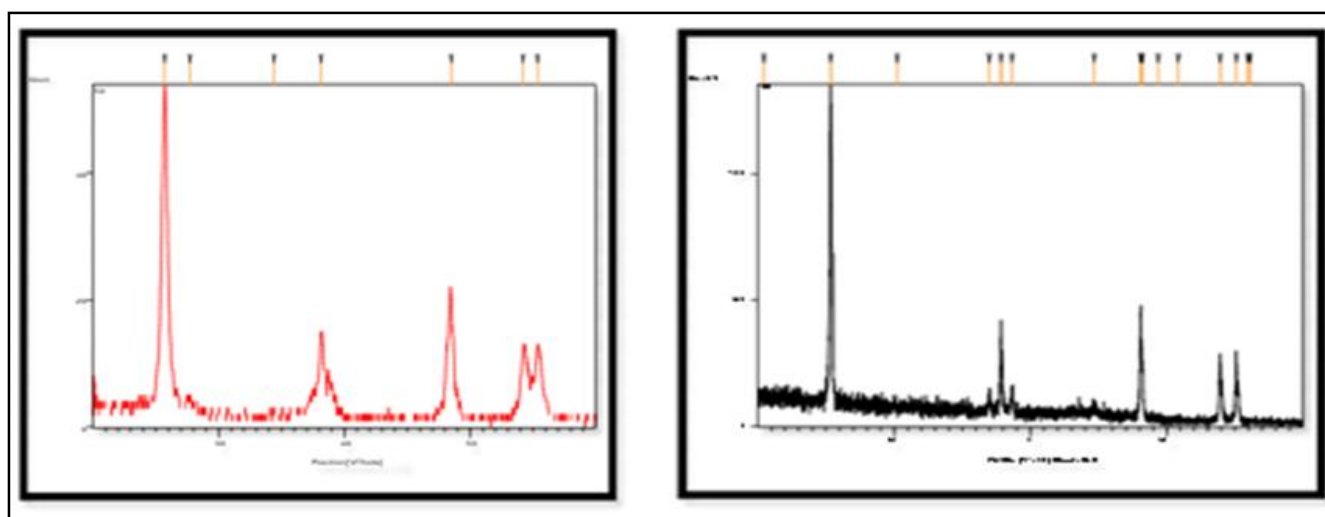


Fig. 2: (2-a) XRD outline for TiO_2 (anatase) while (2-b) XRD outline for Pt.- doped with TiO_2 .

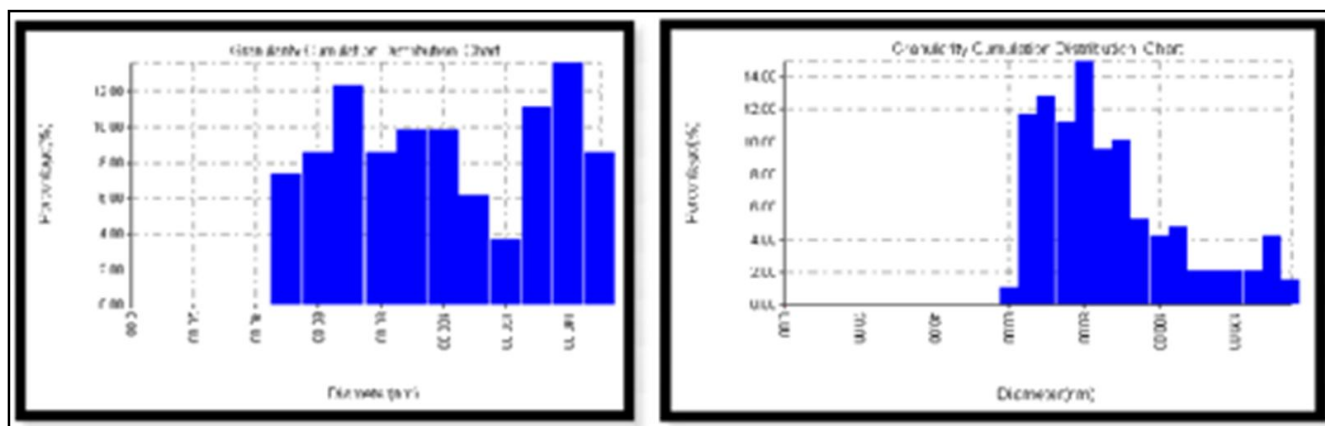


Fig. 3-a: Shown the size distribution for catalyst TiO_2 (anatase) composite AFM,(-b) size distribution for catalyst Pt- doped TiO_2 .(b) prepared particles sketched on X-Y axis catalyst Pt- TiO_2 (anatase) by AFM,(c) prepared particles sketched on X-Y-Z axis for catalyst Pt- TiO_2 (anatase) by AFM. (e) prepared particles sketched on X-Y axis catalyst TiO_2 (anatase) by AFM, (f) prepared particles sketched on X-Y-Z axis for catalyst TiO_2 (anatase) by AFM.

spectrum (Kim *et al.*, 2014) as in Fig. 4, which were measured Bandgap depending on the relevance with Planck postulate.

Effect of Catalyst Weight

The influence of TiO₂ stuffing (mass) on the reaction kinetics was also elaborated, initial concentration fixed in phenanthrene by Pt-doped with TiO₂ using the variation of titania precursors; titanium (IV) at (1×10⁻⁴ mol. L⁻¹) this intent the initial ratio photo degradation reaction (at constant initial concentration) was observed with TiO₂ loading. The outcome is demonstrated in table 2. The data are also presented in Fig 4. As an expected path, with expanding TiO₂ passage the initial concentration of photo catalytic disintegration of phenanthrene degradation on their surface was amplified. The initial point of substrate degradation (0.1 g.L⁻¹) predicts that at TiO₂ stacking higher at that point decline and then become consistent at TiO₂ stacking higher than (0.43 g.L⁻¹) Above this stacking the pace of photo degradation continuously diminishes and this may be clarified by the way that, TiO₂ suspension turns out to be more murky to the episode light and subsequently the light ingestion will be constrained distinctly to the principal layers of the photocatalytic blend and the remainder of the arrangement layers don't get light photons. Also, light dissipating at high anatase stacking turns out to be more viable and this abatements the photon power generally consumed by TiO₂.

Followed by checking its absorption spectrum aquatic solution with initial rate point (1×10⁻⁴ mol.L⁻¹) of the

compound has a $\lambda_{max} = 272\text{nm}$ before exposure. A decline in absorbance was seen after the slip by of 5 minutes utilizing the enhanced load of the impetus (0.43 g.L⁻¹); as in Fig. 9.

On the other hand, substituting of the TiO₂ (anatase) by adopted TiO₂ with Platinum has aremar kable reduced of the absorbance in just 2 minutes associated with that of undoped TiO₂ (5 minutes); as in Fig. 5.

Application TiO₂ (anatase) and Pt-doped TiO₂ on photo degradation of phenanthrene compound exposure (UV) source and direct sun light radiation.

UV source Irradiation

The photo catalytic decomposition of phenanthrene exposure UV source/TiO₂ (anatase)

Direct solar radiation

The photo catalytic decomposition of phenanthrene under direct solar radiation/TiO₂ (anatase). A decrease lack in absorbance was noticed after the elapse of 200 minutes using the optimized weight of the catalyst (0.43 g.L⁻¹); as in Fig 5. Decrease in absorbance was noticed after the elapse of 30 minutes using the optimized weight of the catalyst Pt- doped TiO₂ ; as in Fig. 5. The results of photocatalytic activities Fig. 5 and rate constants table 2 of each type of Pt-doped TiO₂ calcined at 600 K, including P25 TiO₂ indicates that Pt-doped TiO₂ using titanium (IV) tetraisopropoxide provided the best catalytic efficiency. It was able to degrade phenanthrene with the highest conversion of 35% and rate constant of 0.057 h⁻¹ because of its crystallinity, morphology and the amount

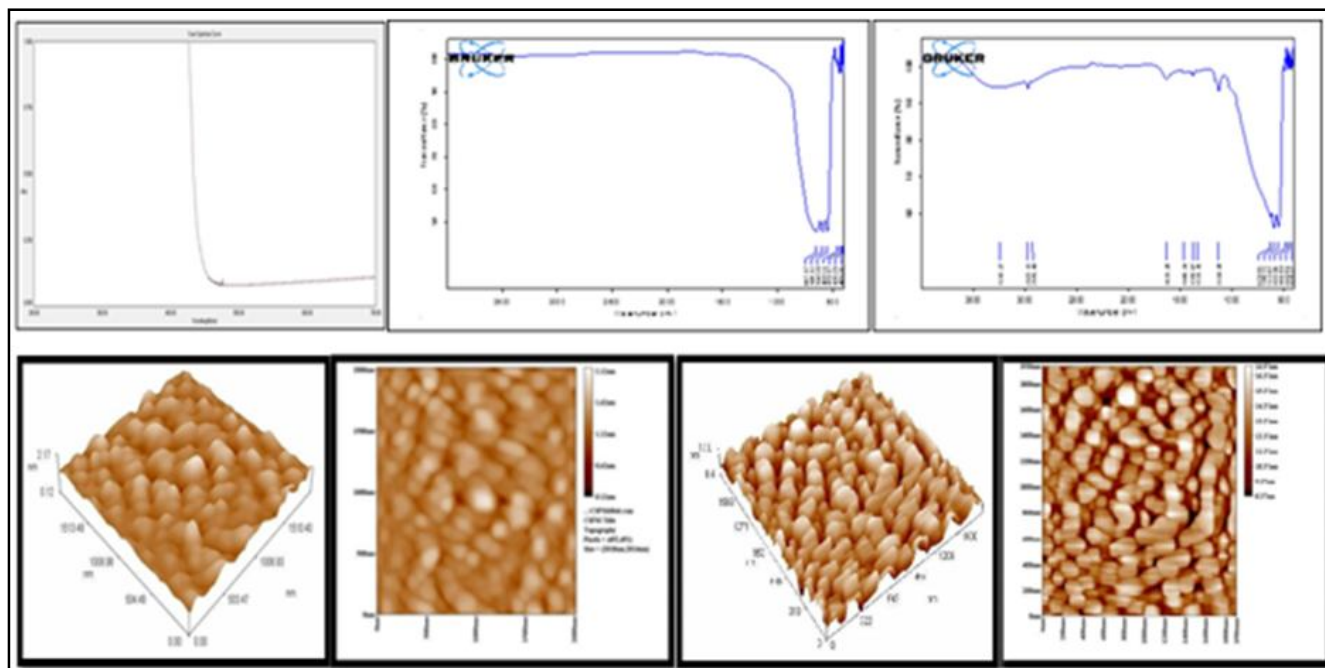


Fig. 4: UV-visible spectra of catalyst Pt- doped TiO₂,ATR-FTIR spectrum of catalyst Pt- doped TiO₂.

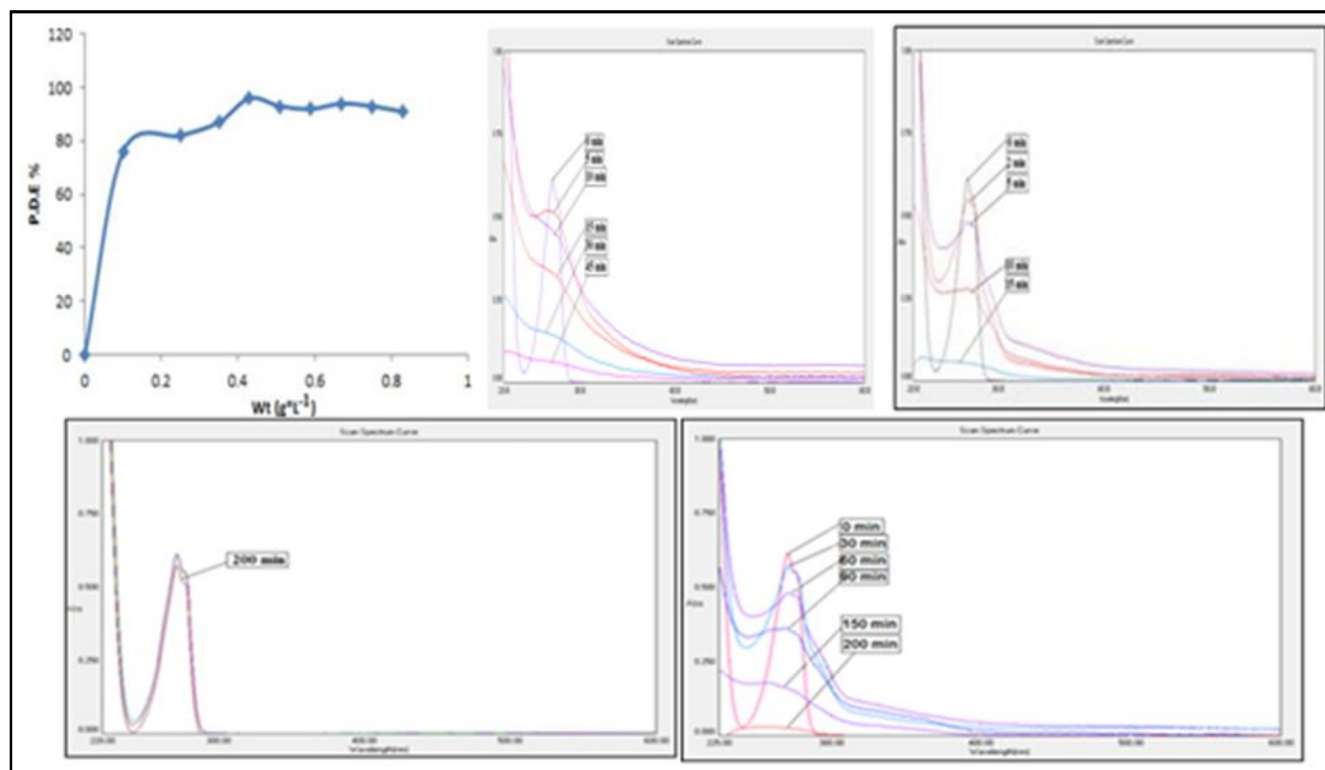


Fig. 5: a) Uv-visible spectra for phenanthrene by catalyst TiO₂ (anatase) under direct solar radiation. b) Uv-visible spectra for phenanthrene by catalyst TiO₂ (anatase) exposed (UV) source, c) Uv-visible spectra of catalyst Pt-doped with TiO₂. d) shown the optimized weight catalyst, UV-visible spectra for phenanthrene by catalyst Pt-doped TiO₂ exposed directly with solar radiation.

of doped Platinum as Ti-Pt. (Bessekhouad, Robert & Weber, 2004; Shi, Zhang & Yao, 2011; Kaewmaraya *et al.*, 2013). Meanwhile, Pt-doped TiO₂ using titanium (IV) tetra-n-butoxide gave 21% conversion of phenanthrene with the rate constant of 0.035 h⁻¹. This result recommends that although it has smaller crystallite size (9.39 nm), its catalytic activity under visible light is not high proportionally because there has been a small amount of strongly-bonded Platinum in its structure. In other words, the 17% conversion and 0.057 h⁻¹ rate constant belongs to Pt-doped TiO₂ using titanium (IV) bis (ethyl acetoacetato) di isopropoxide, indicating that even though this Pt-doped TiO₂ photocatalyst has the high amount of Platinum, its catalytic activity is not enhanced which this outcome goes with (Hu, Song, Jiang & Wei, 2015).

This can be assumed that, firstly, some Platinum species entrapped in TiO₂ are inactive species for photocatalytic degradation such as weakly-adsorbed Platinum species on the surface of TiO₂. Secondly, some parts of the Pt-doped TiO₂ are still amorphous because the XRD peak at 2θ of 25.4° is so broad. Thirdly, the surface morphology has the mixture between fluffy grains and semisolid mass; this result goes with (Sun, & Smirniotis, 2003; Rivas, 2006). The later morphology normally provided the bigger size, which reduced the

specific surface area. Hence, the photocatalytic efficiency is the lowest. Moreover, P25 TiO₂ was also capable of degrading phenanthrene at the 15% conversion of phenanthrene with the rate constant of 0.052 h⁻¹. This phenomenon can be explained by the synergistic interaction between anatase and rutile phases (Connelly, Wahab, & Idriss, 2012). As previous study (Kho *et al.*, 2010), when anatase attached to rutile, it would cause band bending which reduced the possibility of electron-hole recombination. This might enhance the photocatalytic activity of P25 TiO₂. In case of without catalysts, there is no change in the relative concentration of phenanthrene. This result can be implied that all of degraded phenanthrene originated from the photocatalytic reaction rather than the thermal decomposition reaction (Jacob, J. (1996). Besides, under dark reaction in the first one hour, it is evident that the relative concentration of phenanthrene was decreased, suggesting that phenanthrene was physically adsorbed on the surface of Pt-doped TiO₂. After switching the light on, the relative concentration of phenanthrene gradually decreased in case of Pt-doped TiO₂ using titanium (IV) tetra isopropoxide. On the contrary, the other photocatalysts show the increase of the relative concentration of phenanthrene again. This can be implied that Pt-doped TiO₂ using

titanium (IV) tetraisopropoxide was able to degrade phenanthrene immediately that the light was turned on. However, Pt -doped TiO₂ using titanium (IV) tetra-n-butoxide, Pt -doped TiO₂ using titanium (IV) bis (ethyl acetoacetato) disopropoxide and P25 TiO₂ led to the desorption of phenanthrene from their surface rather than sudden degradation of phenanthrene after turning the light on the finding correspondence with (Jacob, 1996; Choi, Stathatos & Dionysiou, 2006). It is inferred that rate of phenanthrene desorption was higher than that of phenanthrene degradation on their surface. After that, they had just abilities to gradually degraded phenanthrene, especially on the last period of degrading time. (Guerin & Jones, 1988; Sokhn, De Leij, Hart & Lynch, 2001; Wen, Zhao, Sheng & Fu, 2003).

References

- Asahi, R.Y.O.J.I., T.A.K.E.S.H.I. Morikawa, T. Ohwaki, K. Aoki and Y. Taga (2001). Visible-light photocatalysis in nitrogen-doped titanium oxides. *Science*, **293(5528)**: 269-271.
- Bessekhouad, Y., D. Robert and J.V. Weber (2004). Bi₂S₃/TiO₂ and CdS/TiO₂ heterojunctions as an available configuration for photocatalytic degradation of organic pollutant. *Journal of Photochemistry and Photobiology A: Chemistry*, **163(3)**: 569-580.
- Bispo, A., M.J. Jourdain and M. Jauzein (1999). Toxicity and genotoxicity of industrial soils polluted by polycyclic aromatic hydrocarbons (PAHs). *Organic Geochemistry*, **30(8)**: 947-952.
- Bozza, F.A., O.G Cruz, S.M. Zagne, E.L. Azeredo, R.M. Nogueira, E.F. Assis and C.F. Kubelka (2008). Multiplex cytokine profile from dengue patients: MIP-1beta and IFN-gamma as predictive factors for severity. *BMC infectious diseases*, **8(1)**: 86.
- Brack, P., S.E. Dann and K.U. Wijayantha (2015). Heterogeneous and homogenous catalysts for hydrogen generation by hydrolysis of aqueous sodium borohydride (NaBH₄) solutions. *Energy Science & Engineering*, **3(3)**: 174-188.
- Chatterjee, D. and S. Dasgupta (2005). Visible light induced photocatalytic degradation of organic pollutants. *Journal of Photochemistry and Photobiology C: Photochemistry Reviews*, **6(2-3)**: 186-205.S.
- Chen, X. and S.S. Mao (2007). Titanium dioxide nanomaterials: synthesis, properties, modifications and applications. *Chemical reviews*, **107(7)**: 2891-2959.
- Choi, H., E. Stathatos and D.D. Dionysiou (2006). Sol-gel preparation of mesoporous photocatalytic TiO₂ films and TiO₂/Al₂O₃ composite membranes for environmental applications. *Applied Catalysis B: Environmental*, **63(1-2)**: 60-67.
- Comini, E., G. Faglia, G. Sberveglieri, Y.X. Li, W. Wlodarski and M.K. Ghantasala (2000). Sensitivity enhancement towards ethanol and methanol of TiO₂ films doped with Pt and Nb. *Sensors and Actuators B: Chemical*, **64(1-3)**: 169-174.
- Connelly, K., A.K. Wahab and H. Idriss (2012). Photoreaction of Au/TiO₂ for hydrogen production from renewables: a review on the synergistic effect between anatase and rutile phases of TiO₂. *Materials for renewable and sustainable energy*, **1(1)**: 3.
- Gaya, U.I. and A.H. Abdullah (2008). Heterogeneous photocatalytic degradation of organic contaminants over titanium dioxide: a review of fundamentals, progress and problems. *Journal of photochemistry and photobiology C: Photochemistry reviews*, **9(1)**: 1-1.
- Godoi, A.F., K. Ravindra, R.H. Godoi, S.J. Andrade, M. Santiago-Silva, L. Van Vaecck and R. Van Grieken (2004). Fast chromatographic determination of polycyclic aromatic hydrocarbons in aerosol samples from sugar cane burning. *Journal of Chromatography A*, **1027(1-2)**: 49-53.
- Guerin, W.F. and G.E. Jones (1988). Two-stage mineralization of phenanthrene by estuarine enrichment cultures. *Applied and Environmental Microbiology*, **54(4)**: 929-936.
- Gust, M.C., L.A. Momoda, N.D. Evans and M.L. Mecartney (2001). Crystallization of Sol-Gel Derived Barium Strontium Titanate Thin Films. *Journal of the American Ceramic Society*, **84(5)**: 1087-1092.
- Hashimoto, K., H. Irie and A. Fujishima (2005). TiO₂ photocatalysis: a historical overview and future prospects. *Japanese journal of applied physics*, **44(12R)**: 8269
- Hu, Y., X. Song, S. Jiang and C. Wei (2015). Enhanced photocatalytic activity of Pt-doped TiO₂ for NO_x oxidation both under UV and visible light irradiation: a synergistic effect of lattice Pt⁴⁺ and surface PtO. *Chemical Engineering Journal*, **274**: 102-112.
- Incardona, J.P., H.L. Day, T.K. Collier and N.L. Scholz (2006). Developmental toxicity of 4-ring polycyclic aromatic hydrocarbons in zebrafish is differentially dependent on AH receptor isoforms and hepatic cytochrome P4501A metabolism. *Toxicology and applied pharmacology*, **217(3)**: 308-321.
- Jacob, J. (1996). The significance of polycyclic aromatic hydrocarbons as environmental carcinogens. *Pure and applied chemistry*, **68(2)**: 301-308.
- Joner, E.J., C. Leyval and J.V. Colpaert (2006). Ectomycorrhizas impede phytoremediation of polycyclic aromatic hydrocarbons (PAHs) both within and beyond the rhizosphere. *Environmental Pollution*, **142(1)**: 34-38.
- Kaewmaraya, T., M. Ramzan, W. Sun, M. Sagynbaeva and R. Ahuja (2013). Atomistic study of promising catalyst and electrode material for memory capacitors: platinum oxides. *Computational materials science*, **79**: 804-810.
- Khan, S.U., M. Al-Shahry and W.B. Ingler (2002). Efficient photochemical water splitting by a chemically modified n-TiO₂. *Science*, **297(5590)**: 2243-2245.
- Kho, Y.K., A. Iwase, W.Y. Teoh, L. Madler, A. Kudo and R. Amal (2010). Photocatalytic H₂ evolution over TiO₂

- nanoparticles. The synergistic effect of anatase and rutile. *The Journal of Physical Chemistry C*, **114(6)**: 2821-2829.
- Kim, W., T. Tachikawa, H. Kim, N. Lakshminarasimhan, P. Murugan, H. Park and W. Choi (2014). Visible light photocatalytic activities of nitrogen and platinum-doped TiO₂: Synergistic effects of co-dopants. *Applied Catalysis B: Environmental*, **147**: 642-650.
- Klosek, S. and D. Raftery (2001). Visible light driven V-doped TiO₂ photocatalyst and its photooxidation of ethanol. *The Journal of Physical Chemistry B*, **105(14)**: 2815-2819R.
- Kryukova, G.N., G.A. Zenkovets, A.A. Shutilov, M. Wilde, K. Günther, D. Fassler and K. Richter (2007). Structural peculiarities of TiO₂ and Pt/TiO₂ catalysts for the photocatalytic oxidation of aqueous solution of Acid Orange 7 Dye upon ultraviolet light. *Applied Catalysis B: Environmental*, **71(3-4)**: 169-176.
- Kumaravel, V., S. Mathew, J. Bartlett and S.C. Pillai (2019). Photocatalytic hydrogen production using metal doped TiO₂: A review of recent advances. *Applied Catalysis B: Environmental*, **244**: 1021-1064.
- Lam, S.M., J.C. Sin and A.R. Mohamed (2008). Recent patents on photocatalysis over nanosized titanium dioxide. *Recent patents on chemical engineering*, **1(3)**: 209-219.
- Li, Q., J. Xue, W. Liang, J.H. Huang and J.K. Shang (2008). Enhanced visible-light absorption in heavily nitrogen-doped TiO₂. *Philosophical magazine letters*, **88(3)**: 231-238.
- Li, X., Q. Liu, X. Jiang and J. Huang (2012). Enhanced photocatalytic activity of Ga-N Co-doped anatase TiO₂ for water decomposition to hydrogen. *Int. J. Electrochem. Sci.*, **7(11)**: 11519-11527.
- Mohapatra, S.K., M. Misra, V.K. Mahajan and K.S. Raja (2007). Design of a highly efficient photoelectrolytic cell for hydrogen generation by water splitting: Application of TiO₂-x C x nanotubes as a photoanode and Pt/TiO₂ nanotubes as a cathode. *The Journal of Physical Chemistry C*, **111(24)**: 8677-8685.
- Nisbet, I.C. and P.K. Lagoy (1992). Toxic equivalency factors (TEFs) for polycyclic aromatic hydrocarbons (PAHs). *Regulatory toxicology and pharmacology*, **16(3)**: 290-300.
- Patil, S.B., P.S. Basavarajappa, N. Ganganagappa, M.S. Jyothi, A.V. Raghu and K.R. Reddy (2019). Recent advances in non-metals-doped TiO₂ nanostructured photocatalysts for visible-light driven hydrogen production, CO₂ reduction and air purification. *International Journal of Hydrogen Energy*, **44(26)**: 13022-13039.
- Li, Q., J. Xue, W. Liang, J.H. Huang, J.F. Guayaquil-Sosa, B. Serrano-Rosales, P.J. Valadés-Pelayo and H. De Lasa (2017). Photocatalytic hydrogen production using mesoporous TiO₂ doped with Pt. *Applied Catalysis B: Environmental*, **211**: 337-348.
- Reszczynska, J., A. Iwulska, G. Sliwinski and A. Zaleska (2012). Characterization and photocatalytic activity of rare earth metal-doped titanium dioxide. *Physicochem. Probl. Miner. Process*, **48(1)**: 201-208.
- Rivas, F.J. (2006). Polycyclic aromatic hydrocarbons sorbed on soils: a short review of chemical oxidation based treatments. *Journal of Hazardous Materials*, **138(2)**: 234-251.
- Sakai, Y.W., K. Obata, K. Hashimoto and H. Irie (2008). Enhancement of visible light-induced hydrophilicity on nitrogen and sulfur-codoped TiO₂ thin films. *Vacuum*, **83(3)**: 683-687H. Irie, Y. Watanabe, K. Hashimoto., *J PhysChem B*, 5483-5486. (2003).
- Shi, Z., X. Zhang and S. Yao (2011). Preparation and photocatalytic activity of TiO₂ nanoparticles co-doped with Fe and La. *Particuology*, **9(3)**: 260-264.
- Sirisaksoontorn, W. (2009). Preparation of N-doped TiO₂ to Use as Catalysts in Photodegradation Reaction of PAHs and Phenol (Doctoral dissertation, Kasetsart University).
- Sokhn, J., F.A.A.M. De Leij, T.D. Hart and J.M. Lynch (2001). Effect of copper on the degradation of phenanthrene by soil micro organisms. *Letters in Applied Microbiology*, **33(2)**: 164-168.
- Souza, J.S. and W.A. Alves (2020). Influence of Preparation Methodology on the Photocatalytic Activity of Nitrogen Doped Titanate and TiO₂ Nanotubes. *Journal of Nanoscience and Nanotechnology*, **20(9)**: 5390-5401.
- Sun, B. and P.G. Smirniotis (2003). Interaction of anatase and rutile TiO₂ particles in aqueous photooxidation. *Catalysis Today*, **88(1-2)**: 49-59.
- Umebayashi, T., T. Yamaki, S. Tanaka and K. Asai (2003). Visible light-induced degradation of methylene blue on S-doped TiO₂. *Chemistry letters*, **32(4)**: 330-331.
- Vela, N., M. Martínez-Menchón, G. Navarro, G. Pérez-Lucas and S. Navarro (2012). Removal of polycyclic aromatic hydrocarbons (PAHs) from groundwater by heterogeneous photocatalysis under natural sunlight. *Journal of Photochemistry and Photobiology A: Chemistry*, **232**: 32-40.
- Wan, X., J. Chen, F. Tian, W. Sun, F. Yang and K. Saiki (2006). Source apportionment of PAHs in atmospheric particulates of Dalian: factor analysis with nonnegative constraints and emission inventory analysis. *Atmospheric Environment*, **40(34)**: 6666-6675.
- Wang, J., F.J. Zhao, A.A. Meharg, A. Raab, J. Feldmann and S.P. McGrath (2002). Mechanisms of arsenic hyperaccumulation in *Pteris vittata*. Uptake kinetics, interactions with phosphate and arsenic speciation. *Plant physiology*, **130(3)**: 1552-1561.
- Wen, S., J. Zhao, G. Sheng and J. Fu (2003). Photocatalytic reactions of pyrene at TiO₂/water interfaces. *Chemosphere*, **50(1)**: 111-119.
- Xie, M.Y., K.Y. Su, X.Y. Peng, R.J. Wu, M. Chavali and W.C. Chang (2017). Hydrogen production by photocatalytic

- water-splitting on Pt-doped $\text{TiO}_2\text{-ZnO}$ under visible light. *Journal of the Taiwan Institute of Chemical Engineers*, **70**: 161-167.
- Yan, J., L. Wang, P.P. Fu and H. Yu (2004). Photomutagenicity of 16 polycyclic aromatic hydrocarbons from the US EPA priority pollutant list. *Mutation Research/Genetic Toxicology and Environmental Mutagenesis*, **557(1)**: 99-108.
- Yin, S., B. Liu, P. Zhang, T. Morikawa, K.I. Yamanaka and T. Sato (2008). Photocatalytic oxidation of NO_x under visible LED light irradiation over nitrogen-doped titania particles with iron or platinum loading. *The Journal of Physical Chemistry C*, **112(32)**: 12425-12431.
- Zhu, Z., C.T. Kao, B.H. Tang, W.C. Chang and R.J. Wu (2016). Efficient hydrogen production by photocatalytic water-splitting using Pt-doped TiO_2 hollow spheres under visible light. *Ceramics International*, **42(6)**: 6749-6754.